

Kinetic Signature of Cooperativity in the Irreversible Collapse of a Polymer

Vittore F. Scolari,^{1,2,*} Guillaume Mercy,^{1,2} Romain Koszul,^{1,2}

Annick Lesne,^{3,4,5} and Julien Mozziconacci^{3,†}

¹*Spatial Regulation of Genomes, Genomes and Genetics Department, Institut Pasteur, Paris 75015, France*

²*UMR3525, Centre National de la Recherche Scientifique, Paris 75015, France*

³*Sorbonne Université, CNRS, Laboratoire de Physique Théorique de la Matière Condensée, LPTMC, Paris F-75252, France*

⁴*Institut de Génétique Moléculaire de Montpellier, UMR 5535 CNRS, Montpellier, France*

⁵*University of Montpellier, Montpellier, France*



(Received 28 November 2017; revised manuscript received 11 April 2018; published 1 August 2018)

We investigate the kinetics of a polymer collapse due to the formation of irreversible cross-links between its monomers. Using the contact probability $P(s)$ as a scale-dependent order parameter depending on the chemical distance s , our simulations show the emergence of a cooperative pearling instability. Namely, the polymer undergoes a sharp conformational transition to a set of absorbing states characterized by a length scale ξ corresponding to the mean pearl size. This length and the transition time depend on the polymer equilibrium dynamics and the cross-linking rate. We confirm experimentally this transition using a DNA conformation capture experiment in yeast.

DOI: [10.1103/PhysRevLett.121.057801](https://doi.org/10.1103/PhysRevLett.121.057801)

The collapse dynamic of a polymer chain has motivated multiple theoretical and experimental investigations [1–10]. The seminal work of de Gennes, considering a collapse caused by solvent quality reduction with no effects of topological constraints, predicted a continuous conformational transition through successive crumpling stages [1]. Grosberg *et al.* proposed a two-stage model, where a fast collapse is followed by a slow unknotting of topological constraints through reptation [2]. The metastable intermediate state, called “fractal globule,” preserves the fractal features of a coil while being compact as a globule. The predicted existence of metastability was experimentally confirmed by Chu *et al.* [3]. The stability of the fractal globule has been investigated in theoretical studies, which quantified the relaxation of this state toward an equilibrium globule [11,12]. As another description of polymer collapse, Buguin *et al.* introduced the concept of pearling through the existence of a characteristic size, there explained by nucleation theory [4]. Pearling has been subsequently studied in different works [5–8,10]. More recently Bunin and Kardar proposed an effective model of polymer collapse consisting of a cascading succession of coalescence events of blobs actively compressed in a central potential [9].

All of these studies investigate the collapse of a polymer under a deep quench: i.e., starting from an equilibrium conformation, interactions between the monomers are abruptly changed and the system relaxes to a new equilibrium state. Memory about the collapse process is lost in this final state. By contrast, we here study the collapse dynamics of a chain when it is caused by the cumulative effect of irreversible cross-links between monomers, in the spirit of the pioneering study by Lifshitz *et al.* [13]. In this case,

cross-links cannot be undone and the final state depends on the collapse dynamics. This process has important applications in materials science (e.g., vulcanization) and in molecular biology (e.g., cell fixation), in particular, recently developed genomewide chromosome conformation capture experiments (Hi-C).

In order to describe the system, we consider here a scale-dependent order parameter: the contact probability curve $P_t(s)$, defined as the mean number of cross-links present at time t between two monomers at a chemical distance s . This order parameter has two important advantages: it reflects the appearance of local structures such as pearls, and it is a direct observable in the Hi-C experiments described at the end of this Letter.

We run a kinetic Monte Carlo simulation [14,15] reproducing the Rouse phenomenology on 2048 beads connected initially by a linear chain of links of maximum length b . Each time two nonlinked beads come in close vicinity (i.e., their distance fall less than $r_{\text{int}} = b/64$), a new link is made with a probability p reflecting the cross-linking rate [details in Sec. IA of the Supplemental Material (SM) [16]]. These links are then treated exactly as the links between consecutive monomers in the chain.

In the absence of cross-linking, the correlations of bead positions along time and along the chain satisfy the Rouse scaling relations with coefficients C_t and C_s [36]:

$$\begin{aligned} \langle |\vec{R}(0, t_0) - \vec{R}(0, t + t_0)|^2 \rangle &\sim C_t t^{1/2}, \\ \langle |\vec{R}(s_0, 0) - \vec{R}(s + s_0, 0)|^2 \rangle &\sim C_s s. \end{aligned} \quad (1)$$

After thermal equilibration of the chain, cross-linking is introduced as a succession of irreversible and

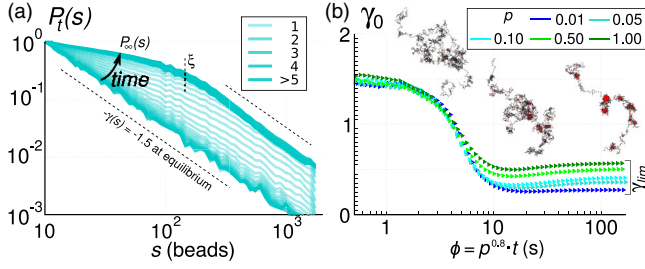


FIG. 1. Kinetics of the pearling transition (simulation). (a) Time evolution of the contact probabilities $P_t(s)$ at fixed cross-link probability $p = 0.1$, displayed as a superposition of semitransparent plots obtained at increasing simulation time t (black arrow); the resulting density is given by the legend. A crossover at length ξ arises at large enough times. Error bars are smaller than the thickness of the line. (b) Evolution of γ_0 , the short-distance exponent of the $P_t(s)$, as a function of the rescaled time ϕ , at different values of p . The fast transition between the original and absorbing states suggests that measured values should follow a bimodal distribution. (Inset) Snapshots of the time evolution of single polymers ($p = 0.1$).

configuration-dependent changes in the chain topology. As a proxy for steric constraints, we limit the cross-link events to a maximum number per bead, N_{\max} , known as the monomer functionality, and stop the simulation once this number is reached for all the beads. N_{\max} is equal to 4 in the figures if not otherwise specified.

Given this dynamics, the contact probability $P_t(s; p, C_s, C_t)$ is a function of s , the cross-link probability p , the Rouse coefficients, and the elapsed time t from the cross-linking onset. At a constant p , the time evolution of this curve displays a transition from the equilibrium contact probability, scaling as $\propto s^{-\gamma}$ with $\gamma = 3/2$ [40], to an asymptotic shape $P_\infty(s)$ displaying a crossover between two different scaling behaviors at short and long chemical distances [Fig. 1(a)]. This shape and the crossover length ξ reflect the population average features of the absorbing states reached by the polymer at cross-link saturation. The exponent $\gamma_0(t)$, corresponding to the value at short distances of the local exponent $\gamma(s; t)$ defined from the discrete differential

$$\gamma(s; t) = -\frac{\Delta \ln[P(s; t)]}{\Delta \ln[s]}, \quad (2)$$

presents a sharp decrease in time [Fig. 1(b), cyan symbols].

We first investigated the effect of the cross-link probability p on the asymptotic curve $P_\infty(s)$ [Fig. 2(a), upper panel]. The crossover length ξ can be estimated as the middle point in the transition of the asymptotic exponent $\gamma_\infty(s)$ from short-distance to large-distance values [Fig. 2(a), lower panel]. This length ξ corresponds to the average length of the polymer segments captured in the pearls, and it will hereafter be referred as the pearling length. The characteristic length ξ could also be recovered from the mean squared distance between monomers as a function of the chemical

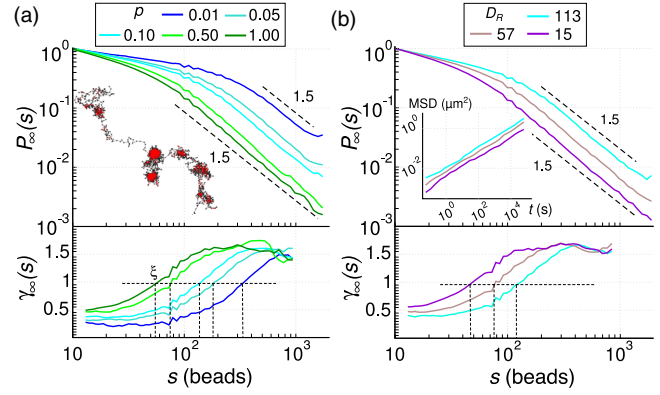


FIG. 2. Quantitative features of the pearling transition (simulation). (a) Asymptotic curve $P_\infty(s)$ (upper panel) and its local slope $\gamma_\infty(s)$ and pearling length ξ (lower panel) for different cross-link probabilities p . (Inset) Example of a pearled state ($p = 0.1$). (b) Asymptotic curve $P_\infty(s)$ (upper panel) and its local slope $\gamma_\infty(s)$ (lower panel) for different polymer dynamics, parametrized by the Rouse coefficient D_R . (Inset) Monomer mean square displacement (MSD) as a function of time. Its intercept yields a measurement of C_t ; see Eq. (1).

distance s (data not shown). Individual pearls were identified by clustering together monomers on the contact graph [41] using the Louvain algorithm [37], and their size was computed in order to confirm that ξ indeed reflects the average number of monomers in pearls (see Fig. 5 of the SM [16]). For $s > \xi$, $\gamma_\infty(s) = 3/2$, consistent with the initial equilibrium state of the polymer, whereas $\gamma_\infty(s)$ tends inside the pearls to a limiting value $\gamma_{\text{lim}} < 1$ at a small enough s .

The length ξ scales with the cross-link probability p as $\xi \propto p^{-\delta}$, with $\delta = 0.4$ [Fig. 3(a)], indicating that the extent along the chain of the cross-link-induced collapse is paradoxically more prominent for small values of p , i.e., a low cross-linking rate. Indeed, conformation changes of polymer loops of size greater than ξ are diffusion limited, while for smaller loops, Rouse diffusion is faster than the cross-linking reaction. In this latter reaction-limited regime, many conformational fluctuations and contacts can occur and be fixed by cross-links, producing pearls of mean size ξ . Based on this qualitative picture, we propose a mean-field calculation of the dependence of ξ on p . The relaxation time for a fixed loop of size s scales as

$$\tau_R(s) = D_R^{-1} s^2, \quad \text{with} \quad D_R = \frac{\pi^3}{4} \left(\frac{C_t}{C_s} \right)^2 \quad (3)$$

(derivation in Sec. II E 4 of the SM [16]), while the average duration τ_{cross} needed to cross link contacting beads is inversely proportional to the cross-link probability: $\tau_{\text{cross}} \propto p^{-1}$. Writing that the pearling length ξ emerges from the competition between these two dynamical processes yields

$$\xi(p) \propto p^{-\delta}, \quad (4)$$

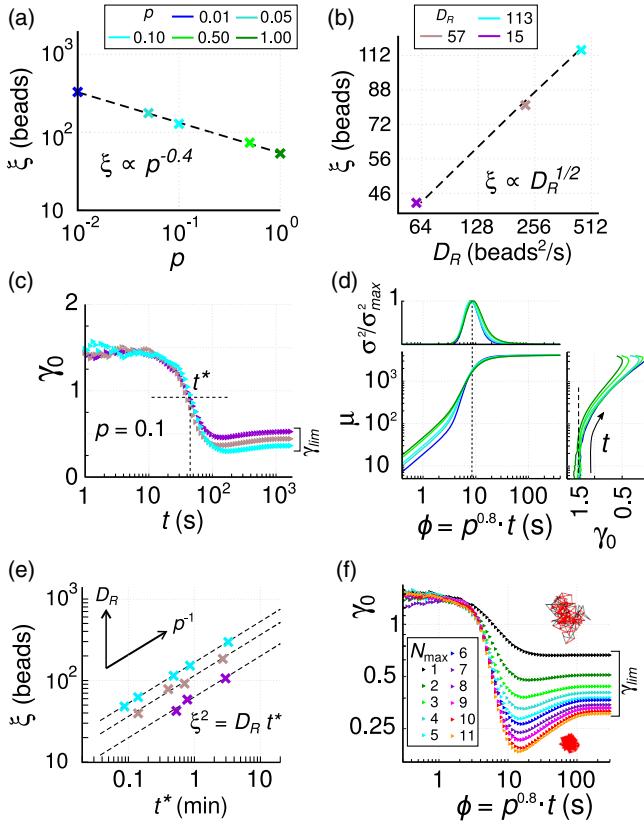


FIG. 3. Dependence of the transition dynamics on the kinetic parameters (simulation). (a) Variation of the pearling length ξ with the cross-link probability p . (b) Variation of the pearling length ξ with the Rouse coefficient D_R . (c) Time evolution of γ_0 at different values of D_R . Equation (3) at a fixed $p = 0.1$. (d) Mean cumulative number μ of cross-link events (lower panel) and its normalized variance σ^2/σ_{\max}^2 (upper panel) as a function of ϕ , and scatterplot of μ and γ_0 (right panel). (e) Scatterplot of the pearling length ξ and the transition time t^* ; dashed lines are plotted using Eq. (7). (f) Evolution of γ_0 as a function of ϕ for different values of the monomer functionality N_{\max} .

with $\delta = 1/2$ almost quantitatively recapitulating the decrease of ξ at increasing values of p . We here assumed that the dynamics is consistent with Rouse diffusion during the pearling formation and collapse. However, Rouse diffusion is not expected to apply to the mesh into what the initially linear polymer is transformed after enough cross-links, which may explain the different value $\delta = 0.4$ measured in the simulations [Fig. 3(a)]. With the same argument we also predict that ξ varies with the dynamical properties of the polymer. Simulations actually show that variation of the Rouse diffusion coefficient D_R has a dramatic effect on ξ [Fig. 2(b)]. For a small D_R , ξ is small and cross-linking has mostly a local effect. When D_R increases, longer polymer segments can reach their equilibrium conformation between two cross-link events so that ξ becomes larger. In the line of the above calculation, we expect a scaling

$$\xi(D_R) \propto D_R^{1/2}, \quad (5)$$

which is well reproduced in the simulations [Fig. 3(b)].

Our simulation, moreover, shows that the collapse happens abruptly. The short-distance exponent γ_0 presents a sharp decrease at a time t^* , which we call the pearling time. Before this transition ($t \ll t^*$), γ_0 coincides with the exponent at long distances, $3/2$, as expected for an equilibrium state. Only after the transition is a smaller exponent observed, with a limiting value $\gamma_{\lim} < 1$ depending on the kinetic parameters. t^* depends on the cross-link probability with a scaling $t^* \propto p^{-0.8}$ prompting us to define a rescaled variable $\phi = p^{0.8}t$. The evolution of γ_0 as a function of ϕ rescales at any p into a single transition curve [Fig. 1(b)]. The scaling of t^* can also be explained with the above mean-field argument: as t^* is directly related to pearling [see polymer snapshots along the transition curve in Fig. 1(b)], it is equal to the relaxation time of pearls of mean size ξ : $t^* = \tau_R(\xi)$. From Eq. (3),

$$t^* \propto p^{-2\delta}, \quad (6)$$

and $\phi^* = p^{2\delta}t$. As predicted by the above argument and confirmed in the simulation, the transition time does not depend on the Rouse diffusion coefficient D_R [Fig. 3(c)]. The pearling transition is the result of the cooperative effect of multiple cross-links, which takes place only after relaxation of loops with length $s < \xi$. This effect is highlighted in Fig. 3(d), lower panel, which shows the acceleration of cross-link events at the transition. This process is accompanied by the decrease of γ_0 [Fig. 3(d), right panel] and a large increase of cross-link number variability due to the fluctuation in the size and time of pearl formation and consistent with a phase transition [Fig. 3(d), upper panel]. Collecting the results from simulations performed at various values of cross-link probability p and Rouse diffusion coefficient D_R , the transition points in the plane defined by pearling time t^* and pearling length ξ [Fig. 3(e)] satisfy the Rouse scaling relation

$$t^* = D_R^{-1}\xi^2, \quad (7)$$

which fully recapitulates the relationship between these physical quantities. We finally determine the influence of steric constraints on the final state by changing the monomer functionality N_{\max} . While ξ and t^* do not depend on N_{\max} , the pearl formation and final internal conformation do, as shown by the time behavior of γ_0 . After a transition in t^* , this short-distance exponent transiently goes toward 0 for large enough values of N_{\max} before plateauing to an asymptotic value γ_{\lim} varying from 0.3 to 0.7 when N_{\max} varies [see Fig. 3(f) and Fig. 6 of the SM [16]]. Examination of the conformational trajectories shows that this behavior can be explained by a two-stage dynamics taking place after the transition in t^* . The first

stage is the formation of densely connected pearls [in red on the snapshots of Fig. 1(b)] linked by stretched linkers containing fewer monomers. In these pearls, virtually any monomer can contact any other monomer, and γ_0 strongly decreases. A slower process then kicks in: the diffusion-limited crumpling of the stretched linkers between adjacent pearls [see the snapshots in Fig. 3(f)]. In the stretched linkers, mostly adjacent monomers are able to come into proximity; hence, the contribution of the collapse to $P(s)$ is such that γ_0 mildly increases.

In summary, our simulation showed how the interplay between the polymer Rouse dynamics and the rate at which cross-links are made induces a cooperative phase transition to pearled conformations with a characteristic scale ξ . We thus obtained a two-stage pearling kinetics, which has already been described in the literature, with, however, some significant differences in the underlying mechanisms. Our irreversible scenario is not compatible with a simple nucleation and growth process: in the nucleation-inspired model of Buguin *et al.* [4], pearls created with a minimal size of ξ grow continuously until the complete collapse of the polymer. We can also exclude knotting effects: Grosberg *et al.* [2] focused on the role of knots in the conformational relaxation and predicted a dense globule with a fractal dimension of 3 and a relaxation through reptation. By contrast, we neglected volume interactions which are a necessary element for knot stability. To see whether the appearance of a specific length scale depends on the fact that we used a phantom chain, we performed an extra simulation taking explicitly into account steric effects. We found in this case that the pearling dynamics of the transition is unchanged (see Fig. 7 of the SM [16]). We also recovered the local formation of a crumple globulelike state in each pearl with $\gamma_0 = 1$. The emergence of the characteristic length ξ , however, excludes fractality of the absorbing conformations. The scale-dependent behavior observed in our simulation reflects the presence of two different dynamics: reaction-limited pearling at short distances along the chain, and diffusion-limited collapse at large distances.

We supplemented our theoretical scenario with an experimental investigation. Indeed, experimental approaches in chromosome biology have recently been renewed by Hi-C experiments that use a succession of cross-linking, restriction, religation, and sequencing steps to measure contact frequencies along a DNA molecule *in vivo*. This technique centrally exploits the unique opportunity offered by the DNA heteropolymer to have a sequence identifier at each locus and so derive a contact probability curve $P(s)$ from cross-link counts. In the paper introducing Hi-C, Lieberman-Aiden *et al.* [38] fitted the resulting curve with a scaling relation $P(s) \propto s^{-\gamma}$, in the range $(1-10) \times 10^6$ base pairs (bp), with a value of γ close to 1 compatible with a fractal-globule state. However, at shorter scales an exponent of 0.75 has also been reported, and other out-of-equilibrium mechanisms were invoked to explain this value: the tension globule [42] or the

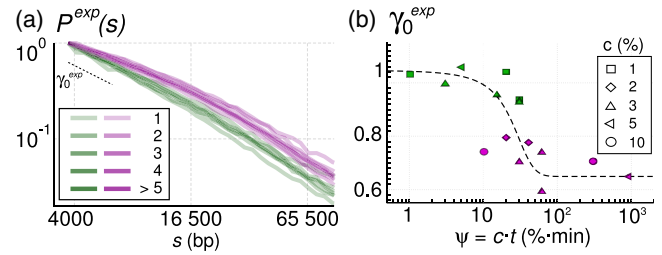


FIG. 4. (a) Experimental contact probability curves $P^{\text{exp}}(s)$ for various cross-linker concentrations c , displayed as a superposition of semitransparent plots [see Fig. 1(a)]. (b) Evolution of the experimental slope γ_0^{exp} as a function of the rescaled time variable $\psi = ct$ [see Fig. 1(b)]. The color discriminates the experiments belonging to the two modalities for γ_0^{exp} , and the dashed line is a guide for the eye.

extrusion of loops by molecular motors [42,43]. While these mechanisms can have a role in chromosome folding, they do not take into account the cross-link-induced distortion caused by the first step of the experiment. This cross-linking step prompted us to exploit Hi-C (methods in Sec. I D of the SM [16] and Refs. [39,44]) to check the collapse scenario described in our simulations. In order to start from configurations that are the closest possible to a simple homopolymer, we used synchronized yeast cells that are neither replicating nor dividing. We performed experiments at different formaldehyde concentrations c and exposure times t to observe the evolution of conformations during the cross-link-induced collapse. Not knowing the reaction order, we cannot establish an exact mapping between k_{on} and c , so we used an ansatz, $\psi = ct$, for the rescaled time variable. The experimental curves $P^{\text{exp}}(s)$ cluster around two different mean curves differing by their slope at short distances γ_0^{exp} [Fig. 4(a)]. Plotting this exponent as a function of ψ , we observe the sharp transition [Fig. 4(b)] predicted by the simulations. Two differences are nevertheless worth discussing. Before the transition, the short-distance exponent of yeast chromosomes is not equal to 1.5 as in the simulations [Fig. 1(b)], but to 1 (0.05 s.d.). This value might either correspond to an effect of volume interactions during the early phases of pearling collapse or to an *in vivo* special organization of the DNA in chromosomes, potentially induced by the regular wrapping of DNA around the nucleosomal protein spools. For distances above 10 000 bp these constraints weaken and the chain follows a typical random walk with an exponent closer to 1.5. After transition, γ_0^{exp} equals 0.7 (0.06 s.d.), corresponding to the value observed for $N_{\text{max}} = 1$ in simulations. This value is likely explained by strong constraints preventing a cross-linked locus to contact other loci. The precise estimation of ξ was impaired by the higher biological and experimental noise on $P^{\text{exp}}(s)$ at increasing distance s , so we could not measure experimentally the dependency of ξ on the cross-linker concentration. Nevertheless, the experiment clearly demonstrates that a polymer experiencing a cross-link-induced

collapse undergoes a sudden transition. It also confirms that inside pearls, at length scales lower than ξ , the conformation in the absorbing state is very compact, with an exponent γ_0 lower than 1, whereas it remains faithful to the original at longer length scales.

Taken together, both our experiments and the simulation evidence a sudden pearling transition in the cross-link-induced collapse of a polymer. This transition involves a characteristic pearl size that is determined by the cross-linking protocol as well as the local dynamics. Our study gives a quantitative description of this transition in time, and of the conformation of the polymer after cross-linking.

We thank Madan Rao, John Marko, Jean-Marc Victor, Benjamin Audit, Marco Cosentino-Lagomarsino, Maxim Dolgushev, and Daniel Jost for the extremely useful discussions and suggestions, and Véronique Legrand and the Information Systems Department (DSI) of Institut Pasteur for the computational power and assistance. This research was supported by funding to R.K. from the European Research Council under the 7th Framework Program (H2020 ERC grant agreement DLV-771813), and by Agence Nationale pour la Recherche (HiResBac ANR-15-CE11-0023-03) to R.K. and J.M.. V.F.S. is recipient of Pasteur-Roux-Cantarini fellowship.

*vittore.scolari@gmail.com

†mozziconacci@lptmc.jussieu.fr

- [1] P. De Gennes, *J. Phys. (Paris), Lett.* **46**, 639 (1985).
- [2] A. Y. Grosberg, S. K. Nechaev, and E. I. Shakhnovich, *J. Phys. (Paris)* **49**, 2095 (1988).
- [3] B. Chu, Q. Ying, and A. Y. Grosberg, *Macromolecules* **28**, 180 (1995).
- [4] A. Buguin, F. Brochard-Wyart, and P. de Gennes, *C.R. Acad. Sci. Ser. Gen., Ser. 2* **322**, 741 (1996).
- [5] B. Ostrovsky, G. Crooks, M. Smith, and Y. Bar-Yam, *Parallel Comput.* **27**, 613 (2001).
- [6] E. Pitard and J.-P. Bouchaud, *Eur. Phys. J. E* **5**, 133 (2001).
- [7] N. V. Dokholyan, E. Pitard, S. V. Buldyrev, and H. E. Stanley, *Phys. Rev. E* **65**, 030801 (2002).
- [8] A. Halperin and P. M. Goldbart, *Phys. Rev. E* **61**, 565 (2000).
- [9] G. Bunin and M. Kardar, *Phys. Rev. Lett.* **115**, 088303 (2015).
- [10] S. Majumder, J. Zierenberg, and W. Janke, *Soft Matter* **13**, 1276 (2017).
- [11] R. D. Schram, G. T. Barkema, and H. Schiessel, *J. Chem. Phys.* **138**, 224901 (2013).
- [12] A. Chertovich and P. Kos, *J. Chem. Phys.* **141**, 134903 (2014).
- [13] I. M. Lifshitz, A. Y. Grosberg, and A. Khokhlov, *ZhETF* **71**, 1634 (1976) [*J. Exp. Theor. Phys.* **44**, 855 (1976)].
- [14] A. Cacciuto and E. Luijten, *Nano Lett.* **6**, 901 (2006).
- [15] V. F. Scolari and M. C. Lagomarsino, *Soft Matter* **11**, 1677 (2015).
- [16] See Supplemental Material at <http://link.aps.org/supplemental/10.1103/PhysRevLett.121.057801>, which includes Refs. [2,14,15,17–39], for supplementary figures and methods.
- [17] A. Amitai and D. Holcman, *Phys. Rev. E* **88**, 052604 (2013).
- [18] J. Bednar, R. A. Horowitz, S. A. Grigoryev, L. M. Carruthers, J. C. Hansen, A. J. Koster, and C. L. Woodcock, *Proc. Natl. Acad. Sci. U.S.A.* **95**, 14173 (1998).
- [19] F. Brochard and P. De Gennes, *J. Phys. (Paris), Lett.* **40**, 399 (1979).
- [20] K. Bystricky, P. Heun, L. Gehlen, J. Langowski, and S. M. Gasser, *Proc. Natl. Acad. Sci. U.S.A.* **101**, 16495 (2004).
- [21] A. Cournac, M. Marbouty, J. Mozziconacci, and R. Koszul, *Methods Mol. Biol. (N.Y.)* **1361**, 227 (2016).
- [22] J. Dekker, K. Rippe, M. Dekker, and N. Kleckner, *Science* **295**, 1306 (2002).
- [23] R. Erban, J. Chapman, and P. Maini, [arXiv:0704.1908](https://arxiv.org/abs/0704.1908).
- [24] A. Y. Grosberg, J.-F. Joanny, W. Srinin, and Y. Rabin, *J. Phys. Chem. B* **120**, 6383 (2016).
- [25] H. Hajjoul, J. Mathon, H. Ranchon, I. Goiffon, J. Mozziconacci, B. Albert, P. Carrivain, J.-M. Victor, O. Gadal, K. Bystricky *et al.*, *Genome Res.* **23**, 1829 (2013).
- [26] E. A. Hoffman, B. L. Frey, L. M. Smith, and D. T. Auble, *J. Biol. Chem.* **290**, 26404 (2015).
- [27] A. Javer, Z. Long, E. Nugent, M. Grisi, K. Siriawatwetchakul, K. D. Dorfman, P. Cicuti, and M. C. Lagomarsino, *Nat. Commun.* **4**, 3003 (2013).
- [28] R. D. Kornberg, *Annu. Rev. Biochem.* **46**, 931 (1977).
- [29] M. Marbouty, C. Ermont, B. Dujon, G.-F. Richard, and R. Koszul, *Yeast* **31**, 159 (2014).
- [30] D. Marenduzzo, C. Micheletti, and P. R. Cook, *Biophys. J.* **90**, 3712 (2006).
- [31] D. Osmanović and Y. Rabin, *Soft Matter* **13**, 963 (2017).
- [32] K. E. Polovnikov, M. Gherardi, M. Cosentino-Lagomarsino, and M. V. Tamm, *Phys. Rev. Lett.* **120**, 088101 (2018).
- [33] S. C. Weber, A. J. Spakowitz, and J. A. Theriot, *Phys. Rev. Lett.* **104**, 238102 (2010).
- [34] S. C. Weber, A. J. Spakowitz, and J. A. Theriot, *Proc. Natl. Acad. Sci. U.S.A.* **109**, 7338 (2012).
- [35] F. B. Wyart and P. De Gennes, *Eur. Phys. J. E* **1**, 93 (2000).
- [36] M. Doi and S. F. Edwards, *The Theory of Polymer Dynamics*, Vol. 73 (Oxford University Press, New York, 1988).
- [37] V. D. Blondel, J.-L. Guillaume, R. Lambiotte, and E. Lefebvre, *J. Stat. Mech.* (2008) P10008.
- [38] E. Lieberman-Aiden, N. L. Van Berkum, L. Williams, M. Imakaev, T. Ragoczy, A. Telling, I. Amit, B. R. Lajoie, P. J. Sabo, M. O. Dorschner *et al.*, *Science* **326**, 289 (2009).
- [39] A. Cournac, H. Marie-Nelly, M. Marbouty, R. Koszul, and J. Mozziconacci, *BMC Genomics* **13**, 436 (2012).
- [40] P.-G. De Gennes, *Scaling Concepts in Polymer Physics* (AIP, Melville, NY, 1980).
- [41] J.-B. Morlot, J. Mozziconacci, and A. Lesne, *Eur. Phys. J. Nonlinear Biomed. Phys.* **4**, 2 (2016).
- [42] A. L. Sanborn, S. S. Rao, S.-C. Huang, N. C. Durand, M. H. Huntley, A. I. Jewett, I. D. Bochkov, D. Chinnappan, A. Cutkosky, J. Li *et al.*, *Proc. Natl. Acad. Sci. U.S.A.* **112**, E6456 (2015).
- [43] G. Fudenberg, M. Imakaev, C. Lu, A. Goloborodko, N. Abdennur, and L. A. Mirny, *Cell Rep.* **15**, 2038 (2016).
- [44] L. Lazar-Stefanita, V. F. Scolari, G. Mercy, H. Muller, T. M. Guérin, A. Thierry, J. Mozziconacci, and R. Koszul, *EMBO J.* **36**, 2684 (2017).